Current Research in Food Science 9 (2024) 100895

Contents lists available at ScienceDirect

Current Research in Food Science

journal homepage: www.sciencedirect.com/journal/current-research-in-food-science

Food processing drives the toxic lectin reduction and bioactive peptide enhancement in *Pinellia ternata*

Xuechun Wang [a,1], Xiqing Bian [b,1], Pingping Dong [b], Li Zhang [a], Lili Zhang [a], Chengfeng Gao [a], Haoyuan Zeng [a], Na Li [a,**], Jian-Lin Wu [a,*]

[a] State Key Laboratory of Quality Research in Chinese Medicine, Macau University of Science and Technology, Taipa, Macau SAR, China
[b] School of Pharmacy, Macau University of Science and Technology, Taipa, Macao SAR, China

ARTICLE INFO

Handling Editor: Dr. Quancai Sun

Keywords:
Pinellia ternata tuber
Processing
Lectins
Bioactive peptides
Antihypertension

ABSTRACT

Processing can change the properties and flavors of food. Many plants in the Araceae family can be used as food or medicine, but their raw materials are usually toxic, such as *Pinellia ternata* tuber (PTT). After processing (processed PTT, PPTT), its toxicity is reduced. However, the mechanism remains unclear. In this study, a novel approach integrating liquid chromatography-mass spectrometry, feature-based molecular networking (FBMN), *de novo* sequencing, and protein database searching was applied to rapidly discover and characterize peptides in PPTT. Potential antihypertensive peptides were screened using *in silico* methods, angiotensin I-converting enzyme (ACE) inhibitory assay, and molecular docking analysis. A significant decrease was observed in toxic lectins after processing. Meanwhile, a total of 1954 mass spectral nodes were discovered in PPTT, of which 130 were annotated as peptides by FBMN. These peptides, ranging from 2 to 21 amino acids, were rapidly identified using PEAKS. Notably, 98 peptides were derived from lectins, most of which increased after processing. Approximately 30% of identified peptides were screened for potential high antihypertensive activity *in silico*. Five peptides exhibited inhibitory effects on ACE, with two showing IC_{50} values of 131 and 185 μM. Dynamic profiling indicated that 7–9 days of processing is optimal for reducing toxicity and enhancing efficacy. More importantly, these peptides were also found in commercial PPTT, confirming their bioactivity contributions. These findings provide insights into the mechanism by which food processing drives the toxic lectin reduction and bioactive peptide enhancement in PTT, providing a novel approach to rapidly discover bioactive peptides, which can be extended to other foods in Araceae family.

1. Introduction

Many plants in the Araceae family can be used as food or medicine; however, most raw species contain varying degrees of toxic compounds such as needle-like calcium oxalate crystals (NCOCs) and lectin proteins (Konozy et al., 2024), which contribute to their toxicity. Therefore, these plants are traditionally processed before use to reduce these toxic components, ensuring they are safe for consumption. *Pinellia ternata* tuber (PTT, Ban xia in Chinese), the dried tuber of *Pinellia ternata* (Thunb.) Breit. (Fam. Araceae), has been widely used in Asian countries for thousands of years (Bai et al., 2022; Tang et al., 2020). It has various activities, such as anti-cough (Tao et al., 2022, 2023), anti-nausea (Zhai et al., 2023), anti-viral (Chen et al., 2020), anti-cancer (Li et al., 2016; Tian et al., 2020), and is traditionally used to eliminate dampness and phlegm, relieve pimple and lose knots (Mao and He, 2020). After processing (processed PTT, PPTT), its toxicity is reduced. Previous studies revealed that processing could decrease the toxicity (Yu et al., 2015) and increase the efficacy of resolving phlegm (Yang et al., 2018). However, the mechanism of efficiency enhancement remains unclear.

Cardiovascular diseases (CVDs) are the leading cause of death all over the world, almost 17.9 million lives die each year. Hypertension is a common clinical disease with high morbidity and mortality (Oparil et al., 2018). It is also a major cause of various CVD (Mills et al., 2020). It is well known that the pathogenesis of hypertension is based on yin deficiency, with yang hyperactivity in the superficiality and phlegm-dampness and blood stasis penetrating all along (Wang and

* Corresponding author.
** Corresponding author.
E-mail addresses: nli@must.edu.mo (N. Li), jlwu@must.edu.mo (J.-L. Wu).
[1] These authors contributed equally to this work.

https://doi.org/10.1016/j.crfs.2024.100895
Received 28 August 2024; Received in revised form 23 October 2024; Accepted 23 October 2024
Available online 24 October 2024

Xiong, 2012). Thus, the activity of eliminating dampness and phlegm of PTT might be associated with antihypertension. Previous studies have demonstrated that PTT has antihypertensive effects (Jiang et al., 2021; Xiong et al., 2012). Nevertheless, the bioactive components of PTT and its mechanism remain to be further investigated.

Liquid chromatography-mass spectrometry (LC-MS) is a widely used ultrasensitive analytical technique that has been increasingly applied to the study of components in food (Dong et al., 2024; Li et al., 2020; Shen et al., 2023). It can provide a wealth of the raw signals including mass-to-charge ratios, retention times, and their intensities. However, transforming raw data into thousands of molecular features and annotating compounds remains a challenging task. Feature-based molecular networking (FBMN) is a powerful analytical approach for rapidly annotating and classifying compounds in GNPS (Nothias et al., 2020). However, the identification of compounds using FBMN relies on the coverage of the MS/MS spectra in the library, which limits the annotation of novel compounds. Fortunately, *de novo* sequencing combined with database search can overcome these limitations and help identify more peptides.

In our study (Fig. 1), an integrated approach, combining liquid chromatography-mass spectrometry (LC-MS), feature-based molecular networking (FBMN), *de novo* sequencing, and protein database search, was applied to rapidly discover and characterize peptides in PPTT. Subsequently, the dynamic changes of toxic lectins and the bioactive peptides were determined. The antihypertensive potential of the bioactive peptides was investigated, and the relationships among the bioactivity, toxicity, and processing days were studied. Moreover, these potential antihypertensive peptides were determined in multiple batches of commercial PTT.

2. Material and methods

2.1. Chemicals and reagents

Peptides including MLFSG, LFSGQVL, VVHPEGRL, VIYGPSVF, and MLFSGQVL were synthesized by Synpeptide Co. Ltd. (Shanghai, China). Bovine serum albumin was purchased from Affymetrix, Inc. (Santa Clara, CA, USA). Acetonitrile (ACN, LC/MS grade) and methanol (MeOH, HPLC grade) were obtained from Anaqua Chemicals Supply Inc., Ltd. (Houston, TA). RIPA lysis buffer, BCA protein assay kit, SDS-PAGE sample loading buffer, 15% SDS-PAGE gel superquick preparation kit, and fast silver stain kit were bought from Beyotime Biotechnology (Beijing, China). Precision plus protein dual color standards were purchased from Bio-Rad (Hercules, CA, USA). Protease and phosphatase inhibitors were bought from Thermo Fisher Scientific Inc. (Massachusetts, USA). Other reagents, including angiotensin I-converting enzyme (ACE, human), hippuryl-l-histidyl-l-leucine (HHL), oxalic acid dihydrate (ACS grade), and formic acid (LC-MS grade), were purchased from Sigma-Aldrich Laboratories, Inc. (St. Louis, MO, USA). Deionized water was prepared using a Millipore water purification system (Millipore, Billerica, MA) with the water outlet operating at 18.2 MΩ.

2.2. Sample preparation

The powder of PTT and PPTT (300 mg) was weighted out in triplicate and extracted successively by 1 mL ACN, 1 mL 50% ACN, and 1 mL of distilled water at room temperature for 1 h. After centrifugation at 15,890 g for 5 min, the supernatants were combined and 50% ACN was added to reach the final volume of 3 mL. The final extracted solution was used for the enrichment of bioactive peptides through MCX cartridges (Chen et al., 2021; Hu et al., 2021). Then, the residues were redissolved in 500 μL MeOH/water (50/50, v/v), and after centrifugation for 5 min at 13,500 rpm, the supernatant was transferred into an HPLC vial and stored at −20 °C prior to use.

2.3. The ultra-high performance liquid chromatography-quadrupole time-of-flight mass spectrometry (UHPLC-Q-TOF/MS) analysis

Samples were analyzed using an Agilent 6545 Accurate-Mass Q-TOF spectrometer coupled to an Agilent 1290 Infinity Binary LC system (UHPLC, Santa Clara, CA, USA) with a Waters ACQUITY UPLC HSS T3 column (2.1 mm × 100 mm, 1.8 μm). The mobile phases were A: 0.1% formic acid in water and B: 0.1% formic acid in ACN. The flow rate was set at 0.3 mL/min. The gradient was set as follows: 0.0–2.5 min, 2.0% B; 2.5–3.0 min, 2.0–10.0% B; 3.0–4.5 min, 10.0–16.0% B; 4.5–10.0 min, 16.0–30.0% B; 10.0–13.0 min, 30.0–95.0% B; and 13.0–15.9 min, 95.0% B; 16.0 min, 2.0% B. The post time is 2 min. The total time for the chromatographic analysis was 16.0 min. The column temperature was

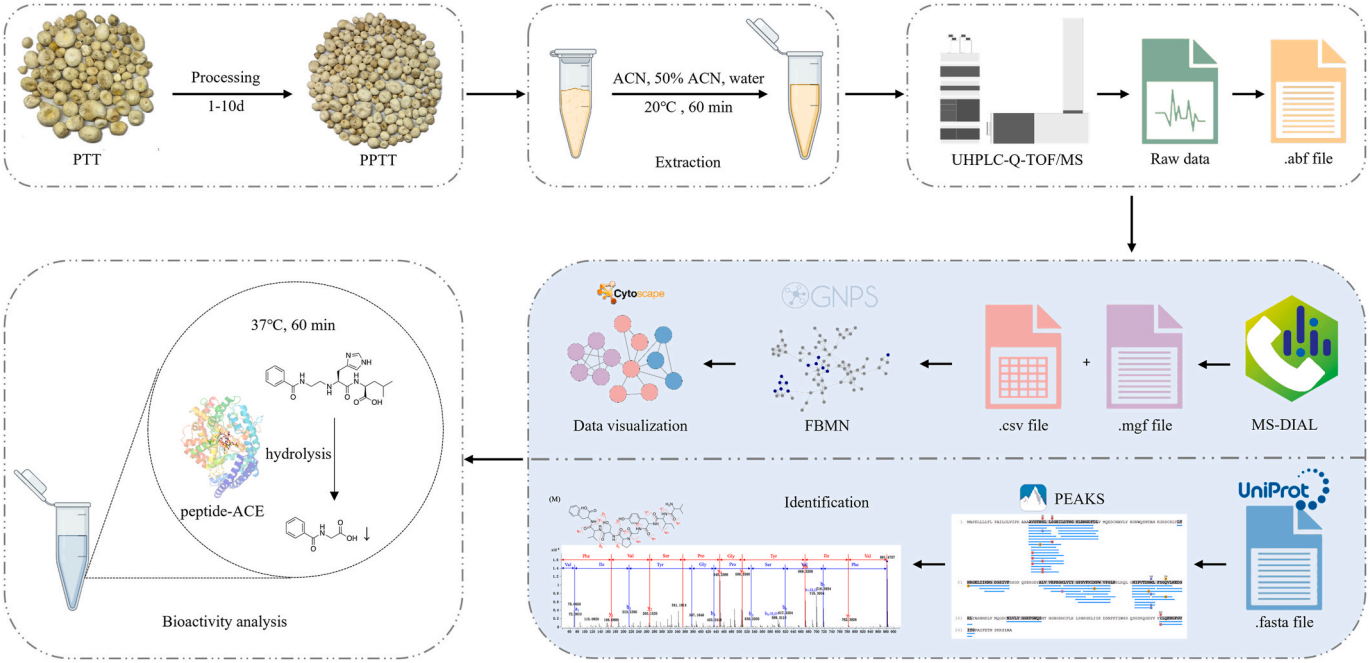

Fig. 1. The workflow of an integrated approach for the discovery of bioactive peptides in PPTT.

maintained at 35 °C and the injection volume was 1 μL.

Electrospray ionization (ESI) was performed in the positive ion mode and the MS parameters were set as follows. Dry gas temperature: 300 °C with a flow of 11 L min^{-1}, sheath gas temperature: 350 °C with a flow of 11 L min^{-1}, nebulizer pressure: 35 psig, capillary voltage: 4000 V, nozzle voltage: 500 V. The mass spectra were recorded across the range of *m/z* 50–1700. Accurate mass measurements were obtained by using a low flow of TOF reference mixture, containing the internal reference mass at *m/z* 922.0098 ($C_{18}H_{18}F_{24}N_3O_6P_3$). Collision-induced dissociation (CID) MS/MS spectra acquisition was performed using automated MS/MS mode, and six intense ions per MS1 scan were selected and subjected to collision-induced dissociation according to the formula: charge 1, slope 3, offset 10 eV; charge 2, slope 1, offset 30 eV [(slope) × (m/z)/100 + offset].

2.4. MS-DIAL data-preprocessing parameters

Reifycs Abf converter (https://www.reifycs.com/AbfConverter/) (X. Wang et al., 2022) was used to convert the raw data file from UHPLC-MS into Abf format. Then, the ABF files are submitted to the metabolomics workflow using MS-DIAL versions 4.80 software with the following parameters set: data collection was performed with 0.01 Da MS1 tolerance and 0.025 Da MS2 tolerance; peak detection was applied with 1000 amplitude for minimum peak height and 0.1 Da for mass slice width. Deconvolution parameters were set as follows: sigma window value of 0.1 and MS/MS abundance cut-off of five amplitudes; retention time tolerance was set as 0.1 min.

2.5. Feature-based molecular networking

After preprocessing the UHPLC-Q-TOF-MS/MS data with MS-DIAL (ver. 4.80), two files were exported for Global Natural Products Social Molecular Networking (GNPS): an mgf file that will be used for molecular networking and the associated Peak Area Quantification Table (a CSV file labeled with "quant" that contains the MS1 peak area abundance information) and uploaded to the GNPS webserver (https://gnps.gucsd.edu) (Gao et al., 2023). The molecular networks were created using the GNPS Featured Based Molecular Networking. After running the spectral clustering algorithm, Cytoscape data was downloaded from the job status pages (https://gnps.ucsd.edu/ProteoSAFe/status.jsp?task=4897bb4e57ec44cabc52b95b5e46087f) and was imported into Cytoscape 3.7.0 software (https://cytoscape.org/) (Chen et al., 2021) along with the feature table for network visualization.

2.6. Construction of annotated protein database

The protein sequence data was downloaded from UniProt database (https://www.uniprot.org/) (Consortium, 2023). All *pinellia ternata* protein entries and trypsin/chymotrypsin inhibitor (Uniprot ID: Q96230) were downloaded in FASTA (canonical) format to create a protein annotation database.

2.7. Peptide and protein identification

The PEAKS® X PRO 10.0 software (Bioinformatics Solutions Inc., Waterloo, Canada) was used to identify peptides and proteins. The general settings were listed as follows: the database was the annotated protein database; precursor mass error tolerance was 10.0 ppm using monoisotopic mass; and fragment ion error tolerance was 0.02 Da; digest mode, unspecific; variable modifications, oxidation (M), acetyl (N-terminus).

2.8. In silico screening of antihypertensive active peptide

The peptides with high antihypertensive activity were predicted using pLM4ACE (https://sqzujiduce.us-east-1.awsapprunner.com/) (Z. Du et al., 2024).

2.9. Assay for ACE inhibitory activity

40 μL of the samples were dissolved in the borate buffer (pH 8.3, 0.1 M, containing 0.3 M NaCl) and 30 μL of ACE solution (0.1 U/mL in borate buffer) were pre-incubated at 37 °C for 10 min. 80 μL of HHL (5 mM in borate buffer) was added to the mixture, and then the mixture was incubated at 37 °C for 60 min. The reaction was terminated by the addition of 200 μL of 1 M HCl. The hippuric acid (HA), produced from the HHL catalyzed by ACE, was extracted with 800 μL ethyl acetate, and dried under a nitrogen stream. The residue was dissolved in 100 μL of 50% MeOH/H_2O and analyzed by a UHPLC system as follows. 5 μL of the mixture was injected into Agilent 1290 Infinity Binary LC system with an Agilent Eclipse Plus-C18 column (2.1 × 100 mm, 1.8 μm). The separation was conducted using an isocratic elution consisting of 75% A (0.1% formic acid in H_2O) −25% B (0.1% formic acid in ACN) at 30 °C and a flow rate of 0.3 mL/min. The detection device was a UV–Vis detector set at 228 nm. The borate buffer was used as a negative control. Triplicate runs were done for each sample. The ACE inhibition ability was calculated as follows:

$$\text{ACE inhibition rate } (\%) = \frac{HA_{control}\text{-}HA_{sample}}{HA_{control}} \times 100$$

where $HA_{control}$ was the peak area of HA in which the tested sample was replaced by the same amount of buffer; HA_{sample} was the peak area of HA with the tested sample. The concentration of peptide required to inhibit 50% of ACE activity was defined as the IC_{50} value.

2.10. Molecular docking with AutoDock vina and PyMOL

In this study, the crystal structure of human angiotensin converting enzyme in complex with lisinopril was downloaded from the Protein Data Bank (https://www.rcsb.org/structure/1O86) (L. Zhang et al., 2022). The protein was prepared by deleting all water molecules and adding all polar hydrogens. The cofactors of zinc atom were retained in the active site, while the lisinopril was deleted. The ChemDraw 3D Pro 14.0 software was used to convert molecule ligands from sdf format to mol2 format. The molecular docking analysis was performed using the AutoDock vina, and the binding affinity of the docked complex was analyzed to choose the best binding mode. The docking output file (.pdbqt) was imported into PyMOL for binding site analysis and protein-ligand interaction visualization.

2.11. Data analysis

The raw data was extracted by Agilent MassHunter Qualitative Analysis B.06.00 software (Agilent Technology, USA). Peak areas were automatically acquired by MS-DIAL. IC_{50} value was calculated with the GraphPad Prism 9. Heatmap was performed through TBtools (version 2.096). All experimental data was expressed in triplicate (n = 3) and processed by GraphPad Prism 9.

3. Results and discussion

3.1. Preparation of PPTT samples

Within the Araceae family, the majority of species are known to produce needle-like calcium oxalate crystals (NCOCs) and lectin proteins, which could cause mucosal irritant toxicity (Chen et al., 2023; Konozy et al., 2024; Peng et al., 2022). Processing is a traditional method to attenuate the toxicity of PTT (Peng et al., 2022; Yu et al., 2015). In our experiments, 3 batches of raw PTT were processed in different days to study the dynamic changes of components during processing. The contents of these toxic components were evaluated and

compared with the commercial PPTT (Fig. 2). Fig. 2A showed a rapid decrease in the levels of NCOCs after 1 day of processing, followed by a gradual decline from 2 to 10 days, ultimately reaching levels comparable to those in commercial PPTT on days 7–10 of processing. Additionally, a notable reduction of lectins (Fig. 2B) was observed after 1 day's processing, followed by a gradual decrease from 1 to 5 days, reaching levels similar to those in commercial PPTT, and remaining almost unchanged when the processing time was extended to 10 days. These results indicated that the PTT samples processed for 7–9 days were suitable for subsequent analysis.

3.2. FBMN analysis of the components in PPTT

It was known that processing had a significant effect on the chemical composition of food (Peng et al., 2022). The levels of components such as organic acids and nucleosides, which were considered to be the main active compounds of PTT, were reported to be decreased after processing (Sun et al., 2019). Thus, other components might contribute to the activity of PTT. Liquid chromatography-mass spectrometry (LC-MS) is a widely used technique for obtaining chemical characteristics of complex components, providing accurate mass-to-charge (m/z) and MS/MS data. However, processing and annotating the acquired data is also a challenging work. Feature-based molecular networking (FBMN) is a powerful analytical approach used in GNPS to explore and annotate complex metabolomic datasets (Nothias et al., 2020). In this research, FBMN method was applied to rapidly discover and characterize the components in PTT.

Initially, the positive ESI mode was chosen for analyzing the components in PTT. LC conditions and MS parameters were optimized to achieve optimal separation of compounds and maximize the acquisition of MS/MS data for each compound. Collision energies were optimized, and a gradient collision energy based on molecular weight was established to enhance the quality of MS/MS spectra. The raw data from LC-MS were converted to abf file format for subsequent analysis using MS-DIAL. Subsequently, the processed data were uploaded to the GNPS online workflow to create molecular networking. Finally, a total of 1954 mass spectral nodes were discovered, and the annotation covered 7 chemical classes, including peptides, amino acids, amines, alkaloids, organic acids, lipids, and polyamines, as shown in Fig. 3A using distinct colors. Among them, 130 special nodes in the first cluster were annotated by FBMN as peptides (Fig. 3A), which have rarely been reported in PTT. Additionally, the abundance and proportion of each peptide in PTT and PPTT were studied and clearly illustrated using pie charts based on the respective extracted ion chromatography (EIC) peak areas (Fig. 3C). These results revealed that the levels of most peptides were significantly increased after processing. Most importantly, the total content of 130 peptides was gradually increased and reached the highest content at the 9th processing (Fig. 3D). It has been reported that peptides possess various activities and the real efficacy of some food may be derived from their bioactive peptides (Liu et al., 2016). We speculated these increased peptides might be associated with the enhanced bioactivity of PTT. Subsequently, further studies on the structures and biological activity of these peptides were conducted in our subsequent investigations.

3.3. Identification of peptides from PPTT

Although the FBMN method accelerated the discovery of peptides, only 16 dipeptides, such as Met-Leu, Thr-Leu, Val-Phe, Val-Leu, Tyr-Tyr, and Leu-Phe, matched the spectra in the GNPS library as shown in Fig. 3B. Nonetheless, characterizing such a large number of nodes remained challenging and time-consuming. PEAKS was a software for sensitive and accurate peptide identification through a combination of *de novo* sequencing and database search techniques (Ma et al., 2003; Zhang et al., 2012). To further expedite the identification of peptides, their MS/MS spectra were imported into PEAKS and a *de novo* sequencing approach was employed to determine the sequences of peptides utilizing the knowledge of the CID fragmentation patterns. This approach gave scores based on the identification of the diagnostic ions, such as the b and y series, and ions from the losses of ammonia or water. In this way, the lengths of all 130 peptides (Fig. 4A, Table S2) were successfully sequenced ranging from 2 to 21 amino acids with high scores (>80 points).

However, a significant challenge in *de novo* sequencing of CID was the inability to distinguish between isomeric amino acid residues, such as Leu/Ile. Thus, we adopted a database-dependent identification strategy by establishing a PTT protein database and matching the high-confidence peptides to it. Briefly, the PTT protein database (Table S1) was constructed containing all entries of "*pinellia ternata*" in UniProt and trypsin/chymotrypsin inhibitor because of its 78% sequence similarity with protease inhibitor, which was also reported as the main protein of PTT (C. Wang et al., 2022; Zhou, 2014). This strategy ensures comprehensive coverage of the peptide originated from the potential protein in PPTT, thereby enhancing the accuracy and reliability of peptide identification. Finally, 98 high-confidence peptides (Fig. 4A) were identified, and all were matched to lectins. However, only 40 peptides with longer than 7 amino acids in length could be matched to proteins using PEAKS. Others were supplemented by manual searches in the protein database, and 58 peptides ranging from 2 to 6 amino acids in length were successfully identified. The number of peptides identified by FBMN, *de novo* sequencing, and protein database searching was shown in Fig. 4A.

To further confirm the structures of the peptides from either lectins or other sources, the MS/MS spectra of the representative peptides were elucidated (Fig. S1), and the standards of some of the peptides were synthesized as comparison. For example, the tetrapeptide LFSG (Fig. S1A) showed the protonated molecular ions $[M+H]^+$ at m/z 423.2238 with the chemical composition of $C_{20}H_{30}N_4O_6$. The fragmentation ions at m/z 86.09 ($[Leu/Ile–H_2O–CO + H]^+$, a_1 ion) and 76.03 ($[Gly + H]^+$, y_1 ion) suggested the presence of the Leu/Ile residue in N-terminal and Gly residue in C-terminal, respectively. In addition, the fragment of m/z 120.0813 (immonium ion $NH_2{=}CHR^+$ of Phe) was

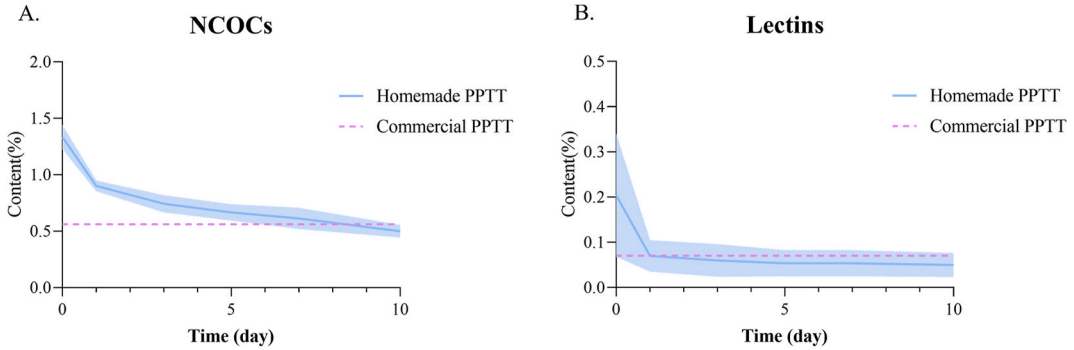

Fig. 2. The dynamic changes of NCOCs (A) and lectins (B) in PTT during processing.

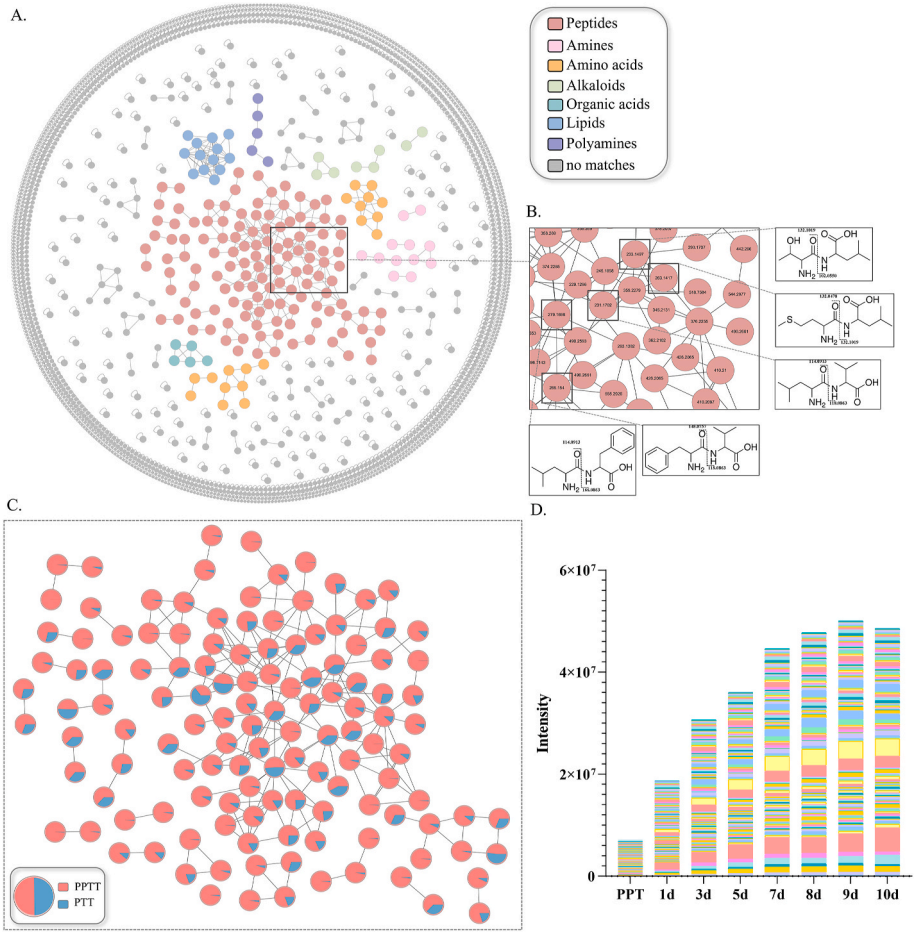

Fig. 3. (A) FBMN and compound class annotations for PTT after processing for 7 days; (B) Dipeptides were identified by matching the spectra in the GNPS library; (C) The relative abundance of each peptide in PTT and PPTT with a pie chart diagram; (D) The dynamic changes of the total content of 130 peptides.

indicative of the Phe residue. Furthermore, the fragments with *m/z* of 261.15 ([Leu/Ile-Phe + H]$^+$, b_2 ion), 233.16 ([Leu/Ile-Phe–CO + H]$^+$, a_2 ion), 348.19 ([Leu/Ile-Phe-Ser + H]$^+$, b_3 ion), 163.07 ([Ser-Gly + H]$^+$, y_2 ion), and 310.13 ([M–Leu/Ile + H]$^+$, y_3 ion) indicated the presence of the Leu/Ile, Phe, Ser, and Gly residues and their binding order. Additionally, by combining with a manual protein database, the Leu and Ile residues were further distinguished, and the peptide was finally confirmed as Leu-Phe-Ser-Gly.

In summary, all 130 peptides (Fig. 4B–Table S2) were successfully characterized, including 20 dipeptides, 41 tripeptides, 7 tetrapeptides, 9 pentapeptides, 3 hexapeptides, 9 heptapeptides, 12 octapeptides, 8 nonapeptides, 4 decapeptides, 2 undecapeptides, 2 tridecapeptides, 2 tetradecapeptides, 2 pentadecapeptide, 2 hexadecapeptides, 1 heptadecapeptide, 4 octadecapeptides, 1 nonadecapeptide, and 1 polypeptide, through a combination of *de novo* sequencing and protein database searching. 98 peptides matching to the lectins were defined as lectin-derived peptides for the first time. Additionally, this integrated strategy enabled the rapid identification of potential bioactive peptides in PPTT and can be applied to other foods in the Araceae family.

3.4. Dynamic changes of the peptides during processing

To comprehensively understand the influence of processing time on peptide generation, the dynamic changes of 130 peptides in PPTT after 1–10 days' processing were monitored and visualized in a heatmap (Fig. 4C). In general, the contents of most peptides increased along with the processing times, especially, most of them reached the highest levels between 7 and 9 days.

Furthermore, it was found that the variations of peptides containing the same short sequences were closely related. For example, 7 peptides with lengths from 3 to 8 (Fig. 4D) containing the sequence "FSG", exhibited a gradual increase in the content, and reached the highest levels at 8 or 9 days of processing. However, except for the tripeptide FSG, the levels of the other 6 longer peptides significantly decreased after 9 days of processing. This phenomenon was also seen in the peptides containing "VIYGPSVF" or "VVHPEGRL" (Fig. 4E) sequences. While VVHPEGRL showed a continuous increase during processing, other peptides containing this sequence, such as VVHPEGRLVIYGPSVF, and ALVVHPEGRLVIYGPSVF, reached peak levels at 8- or 9-days' processing. In addition, VIYGPSVF, VVHPEGKLVIYGPSVF, and ALVVHPEGKLVIYGPSVF exhibited similar increased trends, and reached the highest levels at the 8th and 9th day's processing, followed by a decrease from 9th to 10th day's processing. These phenomena indicated that processing is beneficial for generating more peptides, but the long processing time leads to decrease contents of longer peptides.

3.5. The antihypertensive activity of the peptides in PTT

The bioactivities of peptides are closely related to many factors, such as amino acid sequence, peptide length, and hydrophobicity (Wang et al., 2023). The amino acid sequences of these potential bioactive peptides were analyzed in this study, and it was found that Pro (P), Phe (F), Val (V), and Leu (L) appeared with high frequency at the C-terminus or N-terminus. It was reported that peptides have potential biological activities, especially on the inhibition of angiotensin I-converting enzyme (ACE) (Bas, 2021; L. Zhang et al., 2022). The peptides with

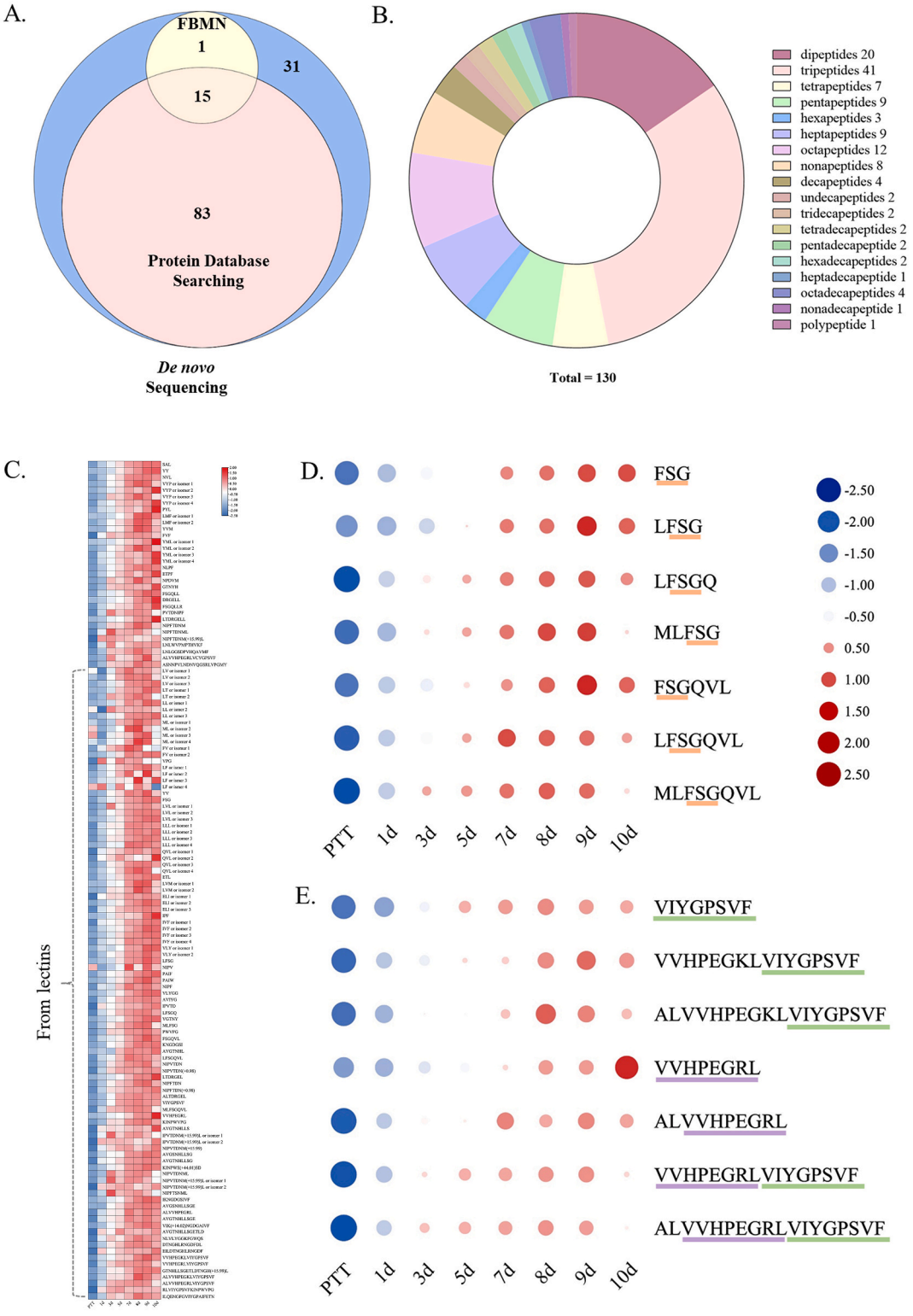

Fig. 4. (A) Venn plot of the number of peptides identified by FBMN, *de novo* sequencing, and protein database searching. (B) Pie chart of the length distribution of the 130 peptides identified in the PPTT. (C) Heatmap of 130 peptides identified from PTT during processing. (D, E) The dynamic changes of the representative peptides in PTT during processing. The levels of peptides are displayed by the color bar, where blue and red respectively represent low and high abundance. The size of circle reflects the degree of color. (For interpretation of the references to color in this figure legend, the reader is referred to the Web version of this article.)

aromatic amino acids (F, Y, and W) or positively charged amino acids (K and R) located at the C-terminal, as well as hydrophobic aliphatic branched chain amino acids (L/I, A, M, and V) or basic amino acids (R, K, and H) located at the N-terminal have been reported to have high ACE-inhibitory capacity (B. Zhang et al., 2022; J. Zhang, L. Liang, L. Zhang et al., 2023). Thus, the activities on antihypertension and ACE were studied in our following study.

3.5.1. *In silico screening of antihypertensive active peptides in PPTT*

The antihypertensive activity of the peptides was evaluated *in silico*

using the pLM4ACE, a protein language model-based deep learning predictor for screening peptides with high antihypertensive activity (Z. Du et al., 2024). All 130 peptides were subjected to pLM4ACE, and approximately 30% (40 peptides) of them were screened for high antihypertensive activity (Fig. 5A, Table S3). Among them, 87.5% (35 peptides) contained specific amino acid residues: Phe (F), Tyr (Y), Trp (W), Lys (K), or Arg (R) located at the C-terminal, and Leu/Ile (L/I), Ala (A), Met (M), Val (V), Arg (R), Lys (K), or His (H) located at the N-terminal. These findings were consistent with previous studies that the peptides with such characteristics exhibited high antihypertensive capacity (J. Zhang, L. Liang, L. Zhang et al., 2023). Subsequently, five representative lectin-derived peptides, including MLFSG, LFSGQVL, MLFSGQVL, VIYGPSVF, and VVHPEGRL, with potential antihypertensive activity *in silico* and higher relative content in PPTT compared with that in PTT (Fig. 5B–F) were synthesized for further investigation.

3.5.2. The ACE inhibitory activity of the peptides

ACE is a potential drug target for the treatment of hypertension, since it plays a vital role in the renin-angiotensin system and converts angiotensin I to angiotensin II (Brown et al., 1998). In our study, five peptides were subjected to ACE inhibitory activity *in vitro*. VIYGPSVF and MLFSG exhibited higher inhibition rates of 69.51% and 80.43%, respectively, at the concentrations of 0.27 and 0.53 mg/mL. Followed by MLFSGQVL, LFSGQVL, and VVHPEGRL, their inhibition rates at the concentration of 1.33 mg/mL were 72.21%, 71.36%, and 53.34%, respectively (Fig. 5G–Table S4). In subsequent experiments, the ACE inhibition activities (IC_{50}) of each peptide were measured and evaluated at 131, 185, 603, 647, and 1140 μM for VIYGPSVF, MLFSG, MLFSGQVL,

Table 1
Inhibitory effects of the 5 lectin-derived peptides on ACE.

No.	Peptides	IC_{50} (μM)
1	VIYGPSVF	131
2	MLFSG	185
3	MLFSGQVL	603
4	LFSGQVL	647
5	VVHPEGRL	1140

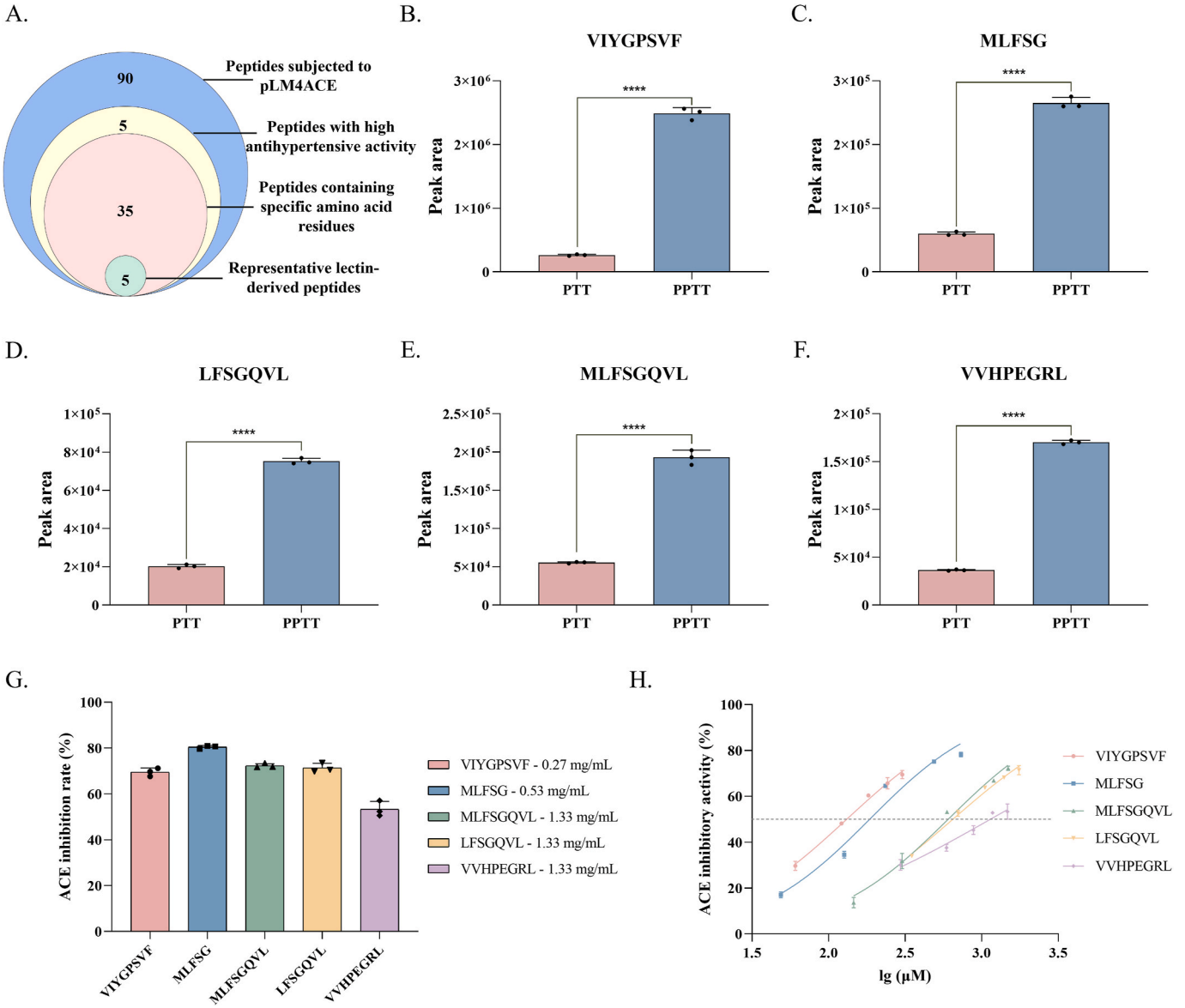

Fig. 5. (A) Venn plot of screening the number of peptides with high antihypertensive activity and containing specific amino acid residues. (B–F) Differences in the content of representative peptides in PTT and PPTT. (G) Inhibitory effects of different concentrations of peptides on ACE. (H) The ACE inhibitory activities (IC_{50}) of each peptide.

LFSGQVL, and VVHPEGRL, respectively (Fig. 5H–Table 1). According to previous reports, peptides with IC_{50} values ranging from 0.32 to 1000 μM had the potential to lower blood pressure (Chen et al., 2022; T. Du et al., 2024). Therefore, these five lectin-derived peptides, especially VIYGPSVF and MLFSG, might contribute to the antihypertensive activity of PPTT. Overall, this integrated approach contributed to the rapid discovery of potential bioactive ingredients in PPTT, which can be extended to other foods in the Araceae family.

3.5.3. Molecular docking analysis of peptides with ACE

To further clarify the mechanisms of ACE inhibition, the 5 peptides were subjected to *in silico* molecular docking. It is known that peptides and ACE residues mainly interacted through hydrogen bonds, hydrophobic interaction, van der Waals, and electrostatic forces, among which the hydrogen bond has the highest frequency (L. Zhang et al., 2022). Previous studies have identified 9 active sites in the 3 active pockets of ACE: S_1 (consisting of residues Ala 354, Glu 384 and Tyr 523), S_2 (including residues Gln 281, His 353, Lys 511, His 513 and Tyr 520) and S_{i} (Glu 162). S_1, S_2, and S_{i} pockets are located at the upper, middle, and lower ends of the ACE, respectively (L. Zhang et al., 2023). The binding energy, number of hydrogen bonds, amino acid residues of ACE enzyme in interaction with the peptide, and H-bond distance were summarized in Table 2.

The results showed that all peptides interacted effectively with ACE (Fig. 6). Specifically, VIYGPSVF, MLFSG, MLFSGQVL, LFSGQVL, and VVHPEGRL exhibited low binding energies of −7.4, −8.2, −6.5, −7.8, and −7.4 kcal/mol, respectively. Briefly, VIYGPSVF (Fig. 6B) formed 6 hydrogen bonds with the ACE enzyme, interacting with residues Ala 354 and Tyr 523 in the S_1 pocket, Tyr 520 and His 513 in the S_2 pocket, and Asp 415, respectively. It has been reported that Ala 354 was an important residue of ACE that interacted with the well-known ACE inhibitor lisinopril (Wang et al., 2023; Zhang et al., 2023), this might explain the high ACE inhibitory activity of VIYGPSVF. Additionally, MLFSG (Fig. 6C) interplayed with S_1 active pocket (Glu 384, Tyr 523), S_2 active pocket (His 353, His 513, Gln 281, Lys 511), $S1'$ active pocket (Glu 162), and Arg 522, *via* 8 hydrogen bonds, respectively. This suggested that MLFSG may effectively interact with residues located at the active site of ACE, which may be the reason for the high ACE inhibitory activity of MLFSG.

Table 2
Molecular docking analysis of 5 lectin-derived peptides with ACE.

No.	Ligand	Binding energy (kcal/mol)	Number of hydrogen bonds (drug-enzyme)	Amino acid residue	H-bond distance (Å)
1	VIYGPSVF	−7.4	6	Ala-354 Asp-415 Tyr-523 Tyr-520 His-513	1.9, 2.6, 2.1, 2.7, 2.2, 2.7
2	MLFSG	−8.2	8	Glu-384 His-353 Arg-522 Tyr-523 His-513 Glu-162 Gln-281 Lys-511	2.6, 2.3, 2.1, 2.1, 2.3, 2.3, 2.3, 2.0
3	MLFSGQVL	−6.5	7	Zn-701 Asp-453 Gln-281 Glu-376 Tyr-523 His-513 Ala-354 His-383	2.3, 2.4, 2.5, 1.9, 2.8, 2.4, 3.2
4	LFSGQVL	−7.8	7	Glu-162 Ala-354 Glu-384 Lys-454 His-353 His-513	2.1, 2.5, 2.1, 2.3, 2.3, 2.3, 2.5
5	VVHPEGRL	−7.4	3	Gln-281 Lys-511 Arg-522	2.4, 1.8, 1.9

3.6. Optimal processing time for PPTT: balancing quality and safety

Food quality is a dominant factor influencing public health and has garnered worldwide attention. Bioactive compounds in food are essential for life, provide health benefits to the human body, and play an important role in assessing food quality (Lili Zhang et al., 2022). Food processing can significantly affect the content of both toxic and active ingredients in PTT. Therefore, it is crucial to optimize food processing methods to ensure food quality and safety. To further determine an appropriate processing time for PPTT in this study, the relationship between these key components and processing days was investigated (Fig. 7). Firstly, antihypertensive peptides such as VIYGPSVF, MLFSGQVL, FSGQVL, and LFSGQVL increased and reached their highest levels on days 7–9 of processing. Conversely, toxic components, including NCOCs and lectin proteins, decreased and reached levels similar to those in commercial PPTT by days 7–10 and 5–10, respectively. In summary, toxic components decreased continuously during processing, while the contents of antihypertensive peptides reached the highest levels at days 7–9 and decreased after 10 days. Considering both the quality and safety of food, a processing time of less than 10 days (e.g., 7–9 days) may be appropriate for PTT to prevent the reduction of bioactive peptides. This finding provides practical recommendations for processing methods to improve the quality and safety of foods in the Araceae family.

3.7. Determination of the bioactive peptides in commercial PPTT

To comprehensively verify the widespread availability of the five bioactive peptides in PPTT, we analyzed 10 batches of commercial PTT from different manufacturers (Table S5). Through LC-MS analysis, all batches of samples were found to contain these five peptides (Fig. S2). These findings revealed that the bioactive peptides identified in our PTT samples were not confined to our study but were common in commercially available PTT products. From another aspect, this observation not only underscored the widespread availability of these bioactive peptides but also highlighted their contributions to the bioactivity of PTT. Such findings facilitate further exploration of the marker compounds responsible for the functionality of PTT, which can be extended to other foods in the Araceae family.

4. Conclusions

In this study, we highlighted an example of how to unveil the mechanism by which food processing drives the toxic lectin reduction and bioactive peptide enhancement in PTT through an integrated approach based on LC-MS, FBMN, *de novo* sequencing, protein database search, and biological activities study. Briefly, 1954 mass spectral nodes were discovered, of which 130 special nodes were annotated as peptides by FBMN. These peptides ranged from 2 to 21 amino acids in length and were rapidly identified in PPTT using PEAKS. Among them, 98 were derived from lectins, most of which increased in content after processing. Bioactivity analysis revealed the potential of lectin-derived peptides as ACE inhibitors, and potentially contributed to the antihypertensive function of PPTT. Furthermore, dynamic profiling indicated that processing is advantageous for reducing toxic lectins and promoting the generation of bioactive peptides. Considering both quality and safety, a processing time of 7–9 days was appropriate for PTT. More importantly, these potential antihypertensive peptides were found in all collected commercial PPTT, indicating their contributions to the bioactivity of PTT from another aspect. Overall, these findings offer valuable insights into the mechanism by which food processing drives the toxic lectin reduction and bioactive peptide enhancement in PTT. Furthermore, this approach could serve as a powerful tool for rapidly discovering bioactive peptides and could be extended to other foods within the Araceae family, thereby improving their safety for consumption.

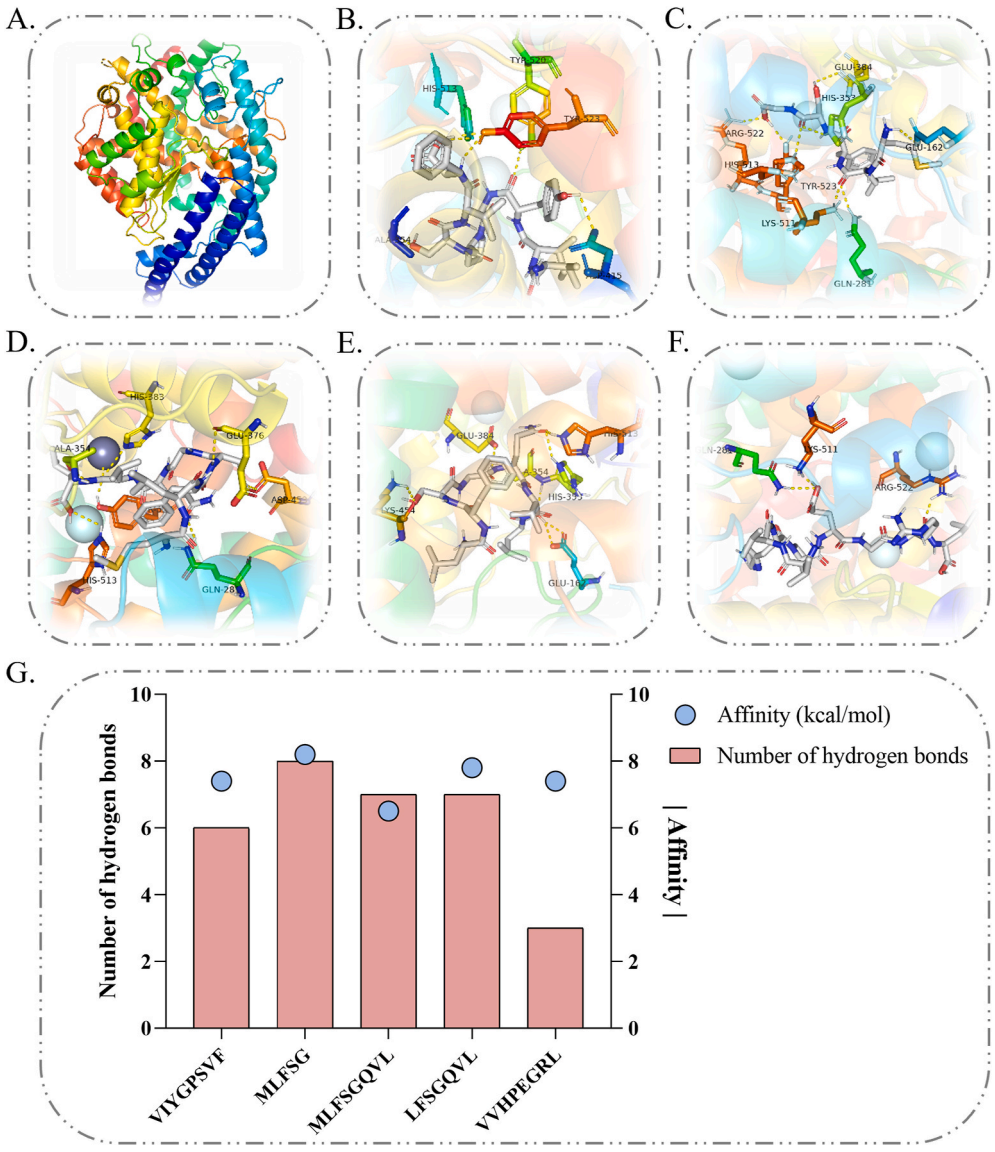

Fig. 6. Molecular docking analysis of bioactive peptides with ACE. A, PDB:1O86; B, VIYGPSVF; C, MLFSG; D, MLFSGQVL; E, LFSGQVL; F, VVHPEGRL; G, The binding energy and number of hydrogen bonds between peptide and ACE.

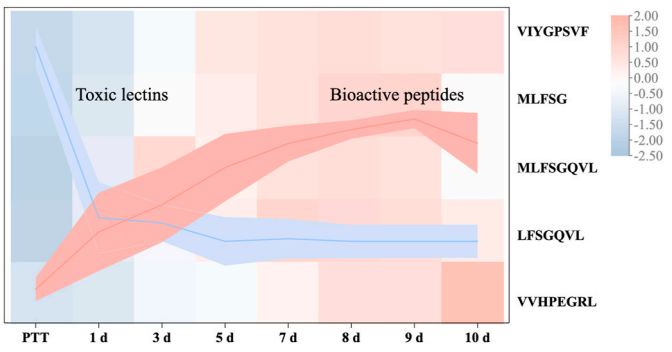

Fig. 7. The dynamic changes of toxic lectins and bioactive peptides during different processing days.

CRediT authorship contribution statement

Xuechun Wang: Writing – original draft, Investigation, Methodology, Software, Data curation. **Xiqing Bian:** Writing – original draft, Validation. **Pingping Dong:** Methodology. **Li Zhang:** Methodology. **Lili Zhang:** Methodology. **Chengfeng Gao:** Methodology. **Haoyuan Zeng:** Methodology. **Na Li:** Writing – review & editing, Supervision. **Jian-Lin Wu:** Conceptualization, Writing – review & editing, Supervision, Supervision.

Declaration of competing interest

The authors declare that they have no known competing financial interests or personal relationships that could have appeared to influence the work reported in this paper.

Acknowledgements

This work was supported by the Science and Technology Development Fund, Macau SAR (file no. FDCT 0001/2020/AKP, 006/2023/SKL, and 0039/2023/ITP1) and Guangxi Science and Technology Major Program (file no. Guike AA22096022).

Appendix A. Supplementary data

Supplementary data to this article can be found online at https://doi.org/10.1016/j.crfs.2024.100895.

Data availability

Data will be made available on request.

References

Bai, J., Qi, J., Yang, L., Wang, Z., Wang, R., Shi, Y., 2022. A comprehensive review on ethnopharmacological, phytochemical, pharmacological and toxicological evaluation, and quality control of Pinellia ternata (Thunb.) Breit. J. Ethnopharmacol. 298, 115650. https://doi.org/10.1016/j.jep.2022.115650.

Bas, Z., 2021. Inhibition effect of nicotinamide (vitamin B(3)) and reduced glutathione (GSH) peptide on angiotensin-converting enzyme activity purified from sheep kidney. Int. J. Biol. Macromol. 189, 65–71. https://doi.org/10.1016/j.ijbiomac.2021.08.109.

Brown, N.J., Vaughan, D.E., 1998. Angiotensin-converting enzyme inhibitors. Circulation 97 (14), 1411–1420. https://doi.org/10.1161/01.cir.97.14.1411.

Chen, C., Sun, Y., Wang, Z., Huang, Z., Zou, Y., Yang, F., Hu, J., Cheng, H., Shen, C., Wang, S., 2023. Pinellia genus: a systematic review of active ingredients, pharmacological effects and action mechanism, toxicological evaluation, and multi-omics application. Gene 870, 147426. https://doi.org/10.1016/j.gene.2023.147426.

Chen, J., Wang, Y.K., Gao, Y., Hu, L.S., Yang, J.W., Wang, J.R., Sun, W.J., Liang, Z.Q., Cao, Y.M., Cao, Y.B., 2020. Protection against COVID-19 injury by qingfei paidu decoction via anti-viral, anti-inflammatory activity and metabolic programming. Biomed. Pharmacother. 129, 110281. https://doi.org/10.1016/j.biopha.2020.110281.

Chen, J., Yu, X., Chen, Q., Wu, Q., He, Q., 2022. Screening and mechanisms of novel angiotensin-I-converting enzyme inhibitory peptides from rabbit meat proteins: a combined in silico and in vitro study. Food Chem. 370, 131070. https://doi.org/10.1016/j.foodchem.2021.131070.

Chen, S., Huang, G., Liao, W., Gong, S., Xiao, J., Bai, J., Wendy Hsiao, W.L., Li, N., Wu, J. L., 2021. Discovery of the bioactive peptides secreted by Bifidobacterium using integrated MCX coupled with LC-MS and feature-based molecular networking. Food Chem. 347, 129008. https://doi.org/10.1016/j.foodchem.2021.129008.

Consortium, T.U., 2023. UniProt: the universal protein knowledgebase in 2023. Nucleic Acids Res. 51 (D1), D523–D531. https://doi.org/10.1093/nar/gkac1052.

Dong, Y., Yan, W., Zhang, Y.Q., Dai, Z.Y., 2024. A novel angiotensin-converting enzyme (ACE) inhibitory peptide from tilapia skin: preparation, identification and its potential antihypertensive mechanism. Food Chem. 430, 137074. https://doi.org/10.1016/j.foodchem.2023.137074.

Du, T., Xu, Y., Xu, X., Xiong, S., Zhang, L., Dong, B., Huang, J., Huang, T., Xiao, M., Xiong, T., Xie, M., 2024. ACE inhibitory peptides from enzymatic hydrolysate of fermented black sesame seed: random forest-based optimization, screening, and molecular docking analysis. Food Chem. 437 (Pt 2), 137921. https://doi.org/10.1016/j.foodchem.2023.137921.

Du, Z., Ding, X., Hsu, W., Munir, A., Xu, Y., Li, Y., 2024. pLM4ACE: a protein language model based predictor for antihypertensive peptide screening. Food Chem. 431, 137162. https://doi.org/10.1016/j.foodchem.2023.137162.

Gao, Y., Fu, Y., Li, N., Jiang, Y., Liu, X., Gao, C., Wang, L., Wu, J.L., Zhou, T., 2023. Carboxyl-containing components delineation via feature-based molecular networking: a key to processing conditions of fermented soybean. Food Chem. 423, 136321. https://doi.org/10.1016/j.foodchem.2023.136321.

Hu, X., Bian, X., Gu, W.Y., Sun, B., Gao, X., Wu, J.L., Li, N., 2021. Stand out from matrix: ultra-sensitive LC-MS/MS method for determination of histamine in complex biological samples using derivatization and solid phase extraction. Talanta 225, 122056. https://doi.org/10.1016/j.talanta.2020.122056.

Jiang, Y.H., Zhang, P., Tao, Y., Liu, Y., Cao, G., Zhou, L., Yang, C.H., 2021. Banxia Baizhu Tianma decoction attenuates obesity-related hypertension. J. Ethnopharmacol. 266, 113453. https://doi.org/10.1016/j.jep.2020.113453.

Konozy, E.H.E., Dirar, A.I., Osman, M.E.M., 2024. Lectins of the Araceae family: insights, distinctions, and future avenues-A three-decade investigation. Biochim. Biophys. Acta Gen. Subj. 1868 (9), 130667. https://doi.org/10.1016/j.bbagen.2024.130667.

Li, S., Tian, Y., Jiang, P., Lin, Y., Liu, X., Yang, H., 2020. Recent advances in the application of metabolomics for food safety control and food quality analyses. Crit. Rev. Food Sci. Nutr. 61 (9), 1448–1469. https://doi.org/10.1080/10408398.2020.1761287.

Li, Y., Li, D., Chen, J., Wang, S., 2016. A polysaccharide from Pinellia ternata inhibits cell proliferation and metastasis in human cholangiocarcinoma cells by targeting of Cdc42 and 67kDa Laminin Receptor (LR). Int. J. Biol. Macromol. 93 (Pt A), 520–525. https://doi.org/10.1016/j.ijbiomac.2016.08.069.

Liu, M., Wang, Y., Liu, Y., Ruan, R., 2016. Bioactive peptides derived from traditional Chinese medicine and traditional Chinese food: a review. Food Res. Int. 89 (Pt 1), 63–73. https://doi.org/10.1016/j.foodres.2016.08.009.

Ma, B., Zhang, K., Hendrie, C., Liang, C., Li, M., Doherty-Kirby, A., Lajoie, G., 2003. PEAKS: powerful software for peptide de novo sequencing by tandem mass spectrometry. Rapid Commun. Mass Spectrom. 17 (20), 2337–2342. https://doi.org/10.1002/rcm.1196.

Mao, R., He, Z., 2020. Pinellia ternata (Thunb.) Breit: a review of its germplasm resources, genetic diversity and active components. J. Ethnopharmacol. 263, 113252. https://doi.org/10.1016/j.jep.2020.113252.

Mills, K.T., Stefanescu, A., He, J., 2020. The global epidemiology of hypertension. Nat. Rev. Nephrol. 16 (4), 223–237. https://doi.org/10.1038/s41581-019-0244-2.

Nothias, L.-F., Petras, D., Schmid, R., Dührkop, K., Rainer, J., Sarvepalli, A., Protsyuk, I., Ernst, M., Tsugawa, H., Fleischauer, M., Aicheler, F., Aksenov, A.A., Alka, O., Allard, P.-M., Barsch, A., Cachet, X., Caraballo-Rodriguez, A.M., Da Silva, R.R., Dang, T., Garg, N., Gauglitz, J.M., Gurevich, A., Isaac, G., Jarmusch, A.K., Kameník, Z., Kang, K.B., Kessler, N., Koester, I., Korf, A., Le Gouellec, A., Ludwig, M., Martin H, C., McCall, L.-I., McSayles, J., Meyer, S.W., Mohimani, H., Morsy, M., Moyne, O., Neumann, S., Neuweger, H., Nguyen, N.H., Nothias-Esposito, M., Paolini, J., Phelan, V.V., Pluskal, T., Quinn, R.A., Rogers, S., Shrestha, B., Tripathi, A., van der Hooft, J.J.J., Vargas, F., Weldon, K.C., Witting, M., Yang, H., Zhang, Z., Zubeil, F., Kohlbacher, O., Böcker, S., Alexandrov, T., Bandeira, N., Wang, M., Dorrestein, P.C., 2020. Feature-based molecular networking in the GNPS analysis environment. Nat. Methods 17 (9), 905–908. https://doi.org/10.1038/s41592-020-0933-6.

Oparil, S., Acelajado, M.C., Bakris, G.L., Berlowitz, D.R., Cifkova, R., Dominiczak, A.F., Grassi, G., Jordan, J., Poulter, N.R., Rodgers, A., Whelton, P.K., 2018. Hypertension. Nat. Rev. Dis. Prim. 4, 18014. https://doi.org/10.1038/nrdp.2018.14.

Peng, W., Li, N., Jiang, E., Zhang, C., Huang, Y., Tan, L., Chen, R., Wu, C., Huang, Q., 2022. A review of traditional and current processing methods used to decrease the toxicity of the rhizome of Pinellia ternata in traditional Chinese medicine. J. Ethnopharmacol. 299, 115696. https://doi.org/10.1016/j.jep.2022.115696.

Shen, S., Zhan, C., Yang, C., Fernie, A.R., Luo, J., 2023. Metabolomics-centered mining of plant metabolic diversity and function: past decade and future perspectives. Mol. Plant 16 (1), 43–63. https://doi.org/10.1016/j.molp.2022.09.007.

Sun, L.M., Zhang, B., Wang, Y.C., He, H.K., Chen, X.G., Wang, S.J., 2019. Metabolomic analysis of raw Pinelliae Rhizoma and its alum-processed products via UPLC-MS and their cytotoxicity. Biomed. Chromatogr. 33 (2), e4411. https://doi.org/10.1002/bmc.4411.

Tang, D., Yan, R., Sun, Y., Kai, G., Chen, K., Li, J., 2020. Material basis, effect, and mechanism of ethanol extract of Pinellia ternata tubers on oxidative stress-induced cell senescence. Phytomedicine 77, 153275. https://doi.org/10.1016/j.phymed.2020.153275.

Tao, X., Li, J., He, J., Jiang, Y., Liu, C., Cao, W., Wu, H., 2023. Pinellia ternata (Thunb.) Breit. attenuates the allergic airway inflammation of cold asthma via inhibiting the activation of TLR4-medicated NF-kB and NLRP3 signaling pathway. J. Ethnopharmacol. 315, 116720. https://doi.org/10.1016/j.jep.2023.116720.

Tao, X., Liu, H., Xia, J., Zeng, P., Wang, H., Xie, Y., Wang, C., Cheng, Y., Li, J., Zhang, X., Zhang, P., Chen, S., Yu, H., Wu, H., 2022. Processed product (Pinelliae Rhizoma Praeparatum) of Pinellia ternata (Thunb.) Breit. Alleviates the allergic airway inflammation of cold phlegm via regulation of PKC/EGFR/MAPK/PI3K-AKT signaling pathway. J. Ethnopharmacol. 295, 115449. https://doi.org/10.1016/j.jep.2022.115449.

Tian, W.T., Zhang, X.W., Liu, H.P., Wen, Y.H., Li, H.R., Gao, J., 2020. Structural characterization of an acid polysaccharide from Pinellia ternata and its induction effect on apoptosis of Hep G2 cells. Int. J. Biol. Macromol. 153, 451–460. https://doi.org/10.1016/j.ijbiomac.2020.02.219.

Wang, C., Bi, Q., Huang, D., Wu, S., Gao, M., Li, Y., Xing, L., Yao, S., Guo, D.A., 2022. Identification of Pinelliae Rhizoma and its counterfeit species based on enzymatic signature peptides from toxic proteins. Phytomedicine 107, 154451. https://doi.org/10.1016/j.phymed.2022.154451.

Wang, J., Shao, B., Li, J., Wang, Z., Zhang, M., Jia, L., Yu, P., Ma, C., 2023. Identification and in silico analysis of ACE-inhibitory peptides derived from milk fermented by lacticaseibacillus paracasei. J. Agric. Food Chem. 71 (33), 12462–12473. https://doi.org/10.1021/acs.jafc.2c09148.

Wang, J., Xiong, X., 2012. Control strategy on hypertension in Chinese medicine. Evid Based Complement Alternat Med 2012, 284847. https://doi.org/10.1155/2012/284847.

Wang, X., Li, N., Chen, S., Ge, Y.H., Xiao, Y., Zhao, M., Wu, J.L., 2022. MS-FINDER assisted in understanding the profile of flavonoids in temporal dimension during the fermentation of Pu-erh tea. J. Agric. Food Chem. 70 (23), 7085–7094. https://doi.org/10.1021/acs.jafc.2c01595.

Xiong, X., Yang, X., Liu, W., Feng, B., Ma, J., Du, X., Wang, P., Chu, F., Li, J., Wang, J., 2012. Banxia baizhu tianma decoction for essential hypertension: a systematic review of randomized controlled trials. Evid Based Complement Alternat Med 2012, 271462. https://doi.org/10.1155/2012/271462.

Yang, B.L.M., Jing, Y., Lai, Y., Liu, J., Peng, L., 2018. Difference of chemical constituents and efficacy between crude and processed *Pinelliae Rhizoma*. Chin. Tradit. Herb. Drugs 49 (18), 4349–4355.

Yu, H., Pan, Y., Wu, H., Ge, X., Zhang, Q., Zhu, F., Cai, B., 2015. The alum-processing mechanism attenuating toxicity of Araceae Pinellia ternata and Pinellia pedatisecta. Arch Pharm. Res. (Seoul) 38 (10), 1810–1821. https://doi.org/10.1007/s12272-015-0556-0.

Zhai, X., He, Q., Chen, M., Yu, L., Tong, C., Chen, Y., Wang, J., Fan, X., Xie, H., Liang, Z., Sui, X., Zeng, L., Wu, Q., 2023. Pinellia ternata-containing traditional Chinese medicine combined with 5-HT3RAs for chemotherapy-induced nausea and vomiting: a PRISMA-compliant systematic review and meta-analysis of 22 RCTs. Phytomedicine 115, 154823. https://doi.org/10.1016/j.phymed.2023.154823.

Zhang, B., Liu, J., Wen, H., Jiang, F., Wang, E., Zhang, T., 2022. Structural requirements and interaction mechanisms of ACE inhibitory peptides: molecular simulation and thermodynamics studies on LAPYK and its modified peptides. Food Sci. Hum. Wellness 11 (6), 1623–1630. https://doi.org/10.1016/j.fshw.2022.06.021.

Zhang, J., Liang, L., Shan, Y., Zhou, X., Sun, B., Liu, Y., Zhang, Y., 2023. Antihypertensive effect, ACE inhibitory activity, and stability of umami peptides from yeast extract. J. Agric. Food Chem. https://doi.org/10.1021/acs.jafc.3c04819.

Zhang, J., Liang, L., Zhang, L., Zhou, X., Sun, B., Zhang, Y., 2023. ACE inhibitory activity and salt-reduction properties of umami peptides from chicken soup. Food Chem. 425, 136480. https://doi.org/10.1016/j.foodchem.2023.136480.

Zhang, J., Xin, L., Shan, B., Chen, W., Xie, M., Yuen, D., Zhang, W., Zhang, Z., Lajoie, G. A., Ma, B., 2012. PEAKS DB: de novo sequencing assisted database search for sensitive and accurate peptide identification. Mol. Cell. Proteomics 11 (4), 010587. https://doi.org/10.1074/mcp.M111.010587. M111.

Zhang, L., Miao, J., Guo, J., Liu, J., Xia, Z., Chen, B., Ma, F., Cao, Y., 2023. Two novel angiotensin I-converting enzyme (ACE) inhibitory peptides from rice (oryza sativa L.) bran protein. J. Agric. Food Chem. 71 (9), 4153–4162. https://doi.org/10.1021/acs.jafc.2c07270.

Zhang, L., Wu, J.L., 2022. Less is more: vital roles of bioactive equivalency in assessing food quality. eFood 3 (6). https://doi.org/10.1002/efd2.49.

Zhang, L., Wu, J.L., Xu, P., Guo, S., Zhou, T., Li, N., 2022. Soy protein degradation drives diversity of amino-containing compounds via Bacillus subtilis natto fermentation. Food Chem. 388, 133034. https://doi.org/10.1016/j.foodchem.2022.133034.

Zhou, Y., 2014. Purification, Expression and Bioactivity Analysis of the Proteins from Pinellia Tenata. Zhejiang Sci-Tech University, Zhejiang.